powder data noted by earlier workers were not found in the present work.

Conclusion

A full solution of the σ phase structure obviously requires very accurate intensity measurements with a small symmetrically shaped crystal to distinguish between the possible space groups and to refine the atomic parameters. In this paper the parameters proposed by Tucker for the β-uranium structure are shown to give reasonably good agreement between observed and calculated structure factors, and it is also suggested that in the Ni–V σ phase there may be a tendency for an ordering of the layer structure to take place. Accurate powder data show that a close correspondence of d values for the various σ phases is found when these are multiplied by appropriate factors, and the structures are therefore completely isomorphous.

The authors would like to thank Dr A. M. B. Douglas for supplying the powder data for the Fe–Cr σ phase and for valuable criticism, Dr G. J. Pitt for helpful advice and Dr W. Hume-Rothery, F. R. S., for his interest in the work.

References

BERGMAN, B. G. & SHOEMAKER, D. P. (1951). *J. Chem. Phys.* **19**, 515.
DICKENS, D. J., DOUGLAS, A. M. B. & TAYLOR, W. H. (1951). *J. Iron Steel Inst.* **167**, 27.
KASPER, J. S., DECKER, B. F. & BELANGER, J. R. (1951). *J. Appl. Phys.* **22**, 361.
TUCKER, C. W. (1951). *Acta Cryst.* **4**, 425.

Acta Cryst. (1952). **5**, 162

A Study of Cold-Worked Aluminium by an X-ray Micro-Beam Technique. I. Measurement of Particle Volume and Misorientations

BY P. B. HIRSCH AND J. N. KELLAR*

Crystallographic Laboratory, Cavendish Laboratory, Cambridge, England

(*Received* 16 *May* 1951 *and in revised form* 17 *June* 1951)

When aluminium is cold-rolled, the original grains break up into smaller particles. X-ray micro-beam back reflexion photographs permit the determination of the mean particle size and misorientation, and of their variation with degree of deformation, time after rolling, and purity of specimen. It is found that for spectroscopically pure aluminium a limiting particle size of $\sim 2\ \mu$ is reached after $\sim 10\ \%$ reduction in thickness, and that the total range of misorientations of the particles in the original grain is several degrees, while the mean angle between neighbouring particles is estimated to be $\sim 2°$. The particle size decreases slightly with time after rolling; for impure aluminium, both the limiting particle size, and the mean angle between adjacent particles are smaller.

1. Introduction

In order to test theories of the strength of polycrystalline metals and to understand the processes of plastic deformation, the structure of the deformed metals must be determined (Bragg, 1948). Heavily deformed metals have been studied by X-ray line-broadening experiments, but the results are difficult to interpret since both small particle-size and strains can contribute to the broadening of the diffraction line. The principle of the present method is to use a micro-beam to reduce the volume of material illuminated to such an extent that spotty diffraction rings are obtained. The mean particle size can be determined from the number of spots on the rings; the shapes of the spots give information on the distortion of the particles. The micro-beam technique has been described elsewhere (Hirsch & Kellar, 1951; Kellar, Hirsch & Thorp, 1950). This paper describes the method for determining the particle volume from the 'spotty' rings, and gives the results obtained for cold-worked aluminium. The interpretation of the spot shapes and a discussion of the results will be presented in later papers.

Spectroscopically pure aluminium was chosen for the first experiments because this material shows small line-broadening even after heavy deformation, so that the particle size must be fairly large ($\sim 10^{-4}$ cm.) even in the heavily cold-worked state (Wood, 1939; Megaw & Stokes, 1945; Paterson, 1949; Hall, 1949). A heavily deformed specimen was used to test the

* This paper describes work carried out in collaboration with the late J. N. Kellar and further work carried out after his death in July 1948.

methods proposed for the interpretation of the back-reflexion micro-beam photographs. Subsequently the structure of aluminium was studied as a function of the degree of cold-work, and time after rolling. The effect of impurities was also investigated.

2. Theory

The mean particle volume is determined from the number of spots on the diffraction rings. Techniques employing this principle have been described for transmission (Schdanow, 1935) and back-reflexion (Stephen & Barnes, 1937) patterns. The present method is a development of the two-exposure method used by Stephen & Barnes. The treatment given below is more general than that used by these authors and leads to a different method for counting spots.

If a beam of monochromatic X-rays of divergence $d\theta$ falls on a perfect particle, a reflexion (at Bragg angle θ) can take place only if the normal to the reflecting planes lies within the volume between two cones of semi-angle $(\frac{1}{2}\pi-\theta)$ and $(\frac{1}{2}\pi-\theta+d\theta)$, with axes along the direction of the incident X-ray beam (Fig. 1). If the incident radiation has a wavelength spread $d\lambda$, the crystal can reflect radiation over a range of angles $d\alpha = \tan\theta d\lambda/\lambda$, and for reflexion to be possible the normal must lie within the volume between two cones of semi-angle $(\frac{1}{2}\pi-\theta)$ and $(\frac{1}{2}\pi-\theta+d\theta+d\alpha)$. If the crystal is bent or strained, or very small, it can reflect radiation over an additional range of angles. The difference between the semi-angles of the two cones can be written as $d\theta+\Delta$, where Δ is equal to the range of angles over which the particle can reflect owing to its imperfections or small size, and owing to the wavelength spread of the radiation.

If the crystals are randomly orientated, the probability of reflexion for a particular particle, for a given set of reflecting planes, is equal to

$$\frac{2\pi\cos\theta(d\theta+\Delta)}{4\pi} = \tfrac{1}{2}\cos\theta(d\theta+\Delta)\,. \qquad (1)$$

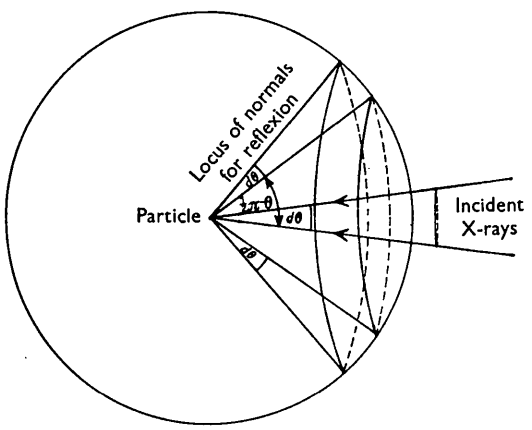

Fig. 1. Diagram illustrating the probability of reflexion of a particle.

If p is the multiplicity factor for the planes, the probability for a particle to reflect at an angle θ is

$$\tfrac{1}{2}p\cos\theta(d\theta+\Delta)\,.$$

If V is the volume of specimen illuminated, and v is the mean volume of particle, the number of reflexions, N, occuring on the particular diffraction ring considered is

$$N = \tfrac{1}{2}(V/v)p\cos\theta(d\theta+\Delta)\,.$$

Now v = area of cross-section (A) × penetration of X-ray beam (l); since l cannot be determined, a two-exposure method is used. If it is assumed that all particles in the specimen are the same size, the intensity of reflexion, I, from a particle at a distance l from the surface is (Fig. 2)

$$I = vKI_0e^{-\mu l(1-\sec 2\theta)},$$

where

I_0 = intensity of incident beam,
K = volume reflexion coefficient for the crystal,
μ = linear absorption coefficient.

Hence, for an exposure T_0, the blackening, B, is

$$B = I.T_0 = vKI_0T_0e^{-\mu l(1-\sec 2\theta)}.$$

Now differences in blackening are due to differences in the depths of the particles below the surface of the specimen. If the only spots counted are those (N_0) with blackening greater than an arbitrary blackening B_0, these are due to reflexions from particles in

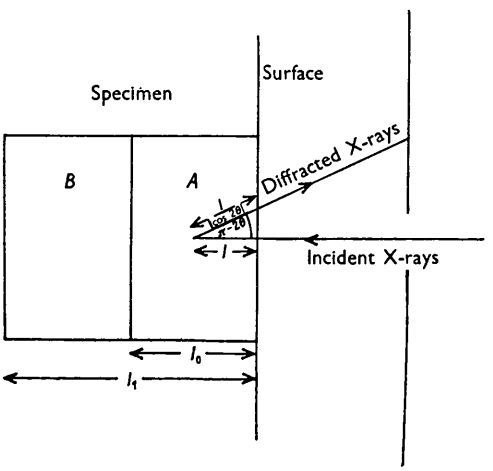

Fig. 2. Diagram illustrating the two-exposure method.

region A (Fig. 2) whose depths below the surface are less than l_0, where

$$l_0 = \frac{1}{\mu(1-\sec 2\theta)}\log\frac{KI_0T_0v}{B_0}\,. \qquad (2)$$

A second exposure, of duration T_1, is taken, and the number of spots with blackening greater than the *same* limiting blackening B_0 is now N_1. The

corresponding penetration of the X-ray beam (region $A+B$ in Fig. 2) is

$$l_1 = \frac{1}{\mu(1-\sec 2\theta)} \log \frac{KI_0T_1v}{B_0} . \quad (3)$$

The difference between the numbers of spots counted in the two cases, N_1-N_0, is due to reflexions from particles in volume B of the specimen, so that

$$N_1-N_0 = \tfrac{1}{2}p \cos\theta(d\theta+\Delta)A(l-l_0)/v$$
$$= \frac{Ap\cos\theta}{2\mu v(1-\sec 2\theta)} \log \frac{T_1}{T_0}(d\theta+\Delta) ,$$

on substitution from (2) and (3). This can be written in the form

$$\frac{N_1-N_0}{A \log_{10} T_1/T_0} = \frac{2{\cdot}3p\cos\theta}{2\mu(1-\sec 2\theta)} \cdot \frac{1}{v} \cdot (d\theta+\Delta) . \quad (4)$$

All variables except v and Δ are known. If several photographs of different divergences are taken, a plot of $\frac{N_1-N_0}{A \log_{10} T_1/T_0}$ against $d\theta$ should be a straight line from the slope of which v can be obtained. This is the basis of the method employed in these experiments.

DISCUSSION OF THEORY

3. Distribution of particle volume

In the above treatment it is assumed that all particles are of the same volume. In practice there is a distribution of volumes in the specimen. Very small particles may give rise to spots which are too weak to be counted. The longer the exposure, the smaller is the limiting volume of a particle giving rise to a spot just sufficiently black for inclusion in the count. For finite exposures the particle size deduced from (4) is always an over-estimate; if, however, the exposures are long, and the limiting blackening is fixed at a sufficiently low level, the number of small particles not taken into account may be negligibly small, so that the particle volume deduced from the experiments is very nearly equal to the mean particle volume.

In this method the exposures are long, the limiting blackening is taken as small as convenient, and the spots on both photographs are counted. In Stephen & Barnes's original method (Stephen & Barnes, 1937) the blackening of the strongest spot on the short-exposure photograph was chosen as the limiting blackening, and spots were counted only on the longer-exposure photograph. Hence, their particle sizes are all over-estimates, as is apparent from Table 1 of their paper, for the estimated grain size decreases with increasing exposure ratio (longer exposures). A full mathematical discussion of the effect of the distribution of particle volumes is given elsewhere (Hirsch, 1950).

4. Preferred orientation

In the derivation of (4) it is assumed that the particles are randomly arranged. In practice, cold-worked specimens usually show preferred orientation. However, the error introduced may not be large, since the particles from which the total number of spots around the ring arises, cover a range of orientations in the specimen. The effect may be minimised by examining a reflexion with a high multiplicity factor; in the experiments on aluminium the 422 reflexion was examined ($p = 24$). The influence of preferred orientation was tested experimentally by examining a specimen in two directions at right angles; the results obtained differed by 20%.

5. Divergence of beam

Since rectangular foci are generally used, the divergence of the beam is not uniform in all directions considered (Hirsch & Kellar, 1951). An average divergence $d\theta_M = (d/r_0)\sqrt{(F/A)}$ is therefore used, where

d = diameter of capillary,
r_0 = distance from capillary to focus,
F = area of foreshortened focus,
A = area of specimen illuminated;

the results so obtained are consistent with equation (4). However, sometimes the size and position of the focus change during the exposure. In that case, the tangential widths of the spots give a direct measure of the average divergence of the beam during the exposure; it will be shown in a later paper that the tangential spot width s_T is given by

$$s_T = \frac{R_0}{|\cos 2\theta|}(d\theta+B_T) ,$$

where B_T is the physical broadening due to distortion and shape of particle, and R_0 is the specimen–film distance.

In terms of s_T, (4) becomes

$$\frac{N_1-N_0}{A \log_{10} T_1/T_0} = \frac{2{\cdot}3p\cos\theta|\cos 2\theta|}{2\mu(1-\sec 2\theta)} \cdot \frac{1}{v} \cdot \left\{\frac{s_T}{R_0} + \frac{\Delta-B_T}{|\cos 2\theta|}\right\} . \quad (5)$$

6. Probability of counting spots

According to equation (4) the intercept of a graph of $\frac{N_1-N_0}{A \log_{10} T_1/T_0}$ against $d\theta$ should be Δ, which is related to the shape and distortion of the particles. However, the method of calculation (§ 2) of the probability of reflexion for a particle includes cases for which the orientation of the particles is such that only a small fraction of the angular divergence of the beam is available for reflexion. These spots may be too small to be counted; experimentally it is found that only spots whose lengths and breadths exceed a

Table 1. *Comparison of counts obtained from different rings*

B_0	${}_1N_{\alpha_1}-{}_1N_{\alpha_2}$	${}_1N_{\alpha_1}-{}_2N_{\alpha_1}$	${}_1N_{\alpha_1}-{}_2N_{\alpha_2}$	$\frac{{}_1N_{\alpha_1}-{}_1N_{\alpha_2}}{\log_{10} T_1/T_0}$	$\frac{{}_1N_{\alpha_2}-{}_2N_{\alpha_1}}{\log_{10} T_1'/T_0}$	$\frac{{}_1N_{\alpha_1}-{}_2N_{\alpha_2}}{\log_{10} T_1''/T_0}$
Large	104	112	160	345·5	296	226
Small	128	174	232	425	430	328

certain fraction of the mean dimensions are included in the measurements. Hence the intercept determined experimentally is less than that expected from the shape and distortion of the particles, and cannot be used to estimate these factors.

If $d\theta$ is large compared with Δ, this factor can be neglected and the mean volume of the particles can be determined from photographs taken with one large value of $d\theta$. More accurate values can be obtained by using equation (5), for the intercept is proportional to $(\Delta - B_T)$, which is less than Δ, and the error incurred in neglecting this term will be smaller.

7. Test of method

Back-reflexion photographs of a specimen of heavily rolled and recovered spectroscopically pure aluminium were taken with micro-beams of $\sim 35\ \mu$ diameter and various divergences between 10^{-3} and 3×10^{-3} radians. For each exposure two films were placed in the film-holder; the α_1 and α_2 rings on both films provided material for four independent counts for known exposure ratios. In the calculation of the exposure ratios, the ratio of the intensity of α_1 and α_2 radiation was assumed to be 2 (Compton & Allison, 1935 chap. 8);

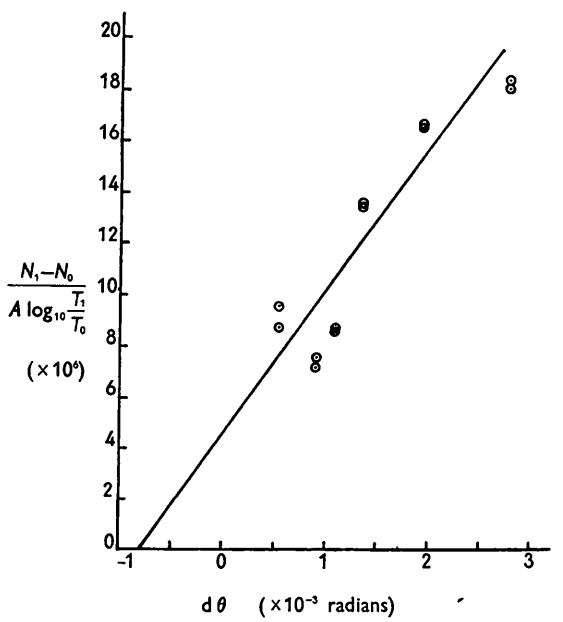

Fig. 3. Experimental points obtained by the method of counting spots for a specimen of heavily rolled and recovered spectroscopically pure aluminium; the pairs of points (obtained as described in § 7) are plotted against the divergence of the beam.

the absorption coefficient of the film was measured and the fraction of the intensity of the diffracted beam (422 reflexion) transmitted by the first film was found to be 1/2·5.

A weak spot on the α_1 ring of the first photograph was chosen to correspond to the limiting blackening B_0. The number of spots on the four rings with blackening greater than B_0 were counted (${}_1N_{\alpha_1}$, ${}_1N_{\alpha_2}$, ${}_2N_{\alpha_1}$, ${}_2N_{\alpha_2}$). Usually ${}_2N_{\alpha_2}$ could not be regarded as reliable, because the spots on the α_2 ring of the second film were weaker than the limiting blackening (cf. § 4). Thus in practice two reliable estimates of the difference between the number of spots could be made (i.e. ${}_1N_{\alpha_1}-{}_1N_{\alpha_2}$; ${}_1N_{\alpha_1}-{}_2N_{\alpha_1}$) and these were to be in the ratio of the logarithms of the exposure ratios. Generally it was found that $\frac{{}_1N_{\alpha_1}-{}_1N_{\alpha_2}}{\log_{10} T_1/T_0}$ was greater than $\frac{{}_1N_{\alpha_1}-{}_2N_{\alpha_1}}{\log_{10} T_1'/T_0}$; it can be shown that this could be expected if B_0 was too large for the α_1 ring on the second photograph (for further details, see Hirsch, 1950). B_0 was then reduced and the count repeated until the figures were nearly equal. All the experimental points were obtained in this way. An example is given in Table 1.

The values 425 and 430 obtained from the counts of ${}_1N_{\alpha_1}$, ${}_1N_{\alpha_2}$ and ${}_2N_{\alpha_1}$ are sufficiently close to be used in the calculation of the mean volume of the particles.

The experimental points are shown in Figs. 3 and 4, plotted against $d\theta$ and s_T/R_0 respectively. The spread of the points on Fig. 4 is smaller, and the particle size $t\ (=v^{\frac{1}{3}})$ obtained from the slope of the straight line fitted to these points is 1·7 μ ($\pm$0·2 μ). The larger systematic error due to preferred orientation was estimated by examining the same specimen at right angles. The value of t obtained was 2·1 μ. Hence the mean value of particle size may be taken as 1·9 μ, the probable accuracy being $\sim \pm 0{\cdot}4\ \mu$.

From the consistency of the results it may be concluded that the formulae can be used as a reasonable working basis for the determination of mean particle size from spotty-ring photographs. The advantage of this method over that depending on line broadening is that the results can be interpreted unambiguously in terms of particle size. A particular feature of the graphs is the small intercept; hence fairly accurate values of t may be obtained from photographs with a large divergence (say $2\text{–}3\times10^{-3}$ radians). All other determinations of particle size for aluminium have been made in this way; the order of magnitude of Δ and the intercept expected could be determined from the broadenings of the spots on a

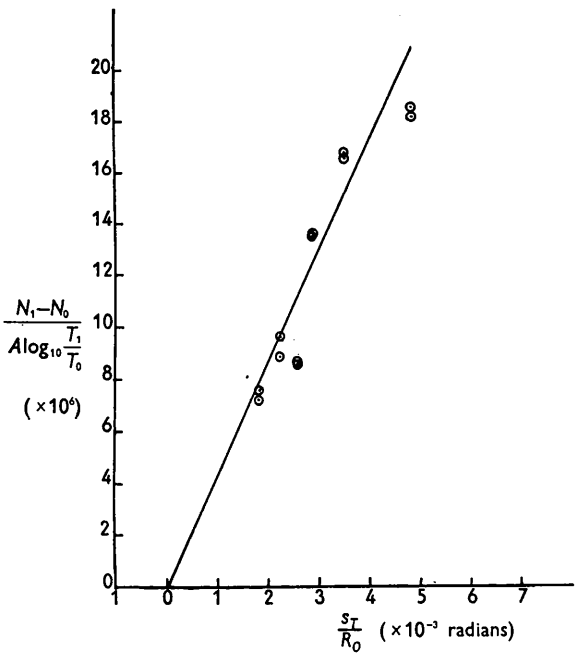

Fig. 4. Results of Fig. 3, plotted against the tangential spot width.

preliminary photograph (see footnote to § 5 of Hirsch, 1952).

RESULTS

8. Particle size and misorientations as a function of deformation

In these experiments specimens of spectroscopically pure aluminium (Johnson and Matthey 99·99 %) were cold-rolled and etched to remove possible surface contaminations, and X-ray photographs were then taken. Fig. 5 shows micro-beam photographs of undeformed and deformed materials; Fig. 6 shows enlarged sections of the photographs for a slightly and a heavily rolled specimen.

After slight rolling the sharp spots on the photographs of the original material spread out into arcs (Fig. 5(*a*), (*b*)). These arcs consist of a number of spots, showing that the grain was broken up into a number of smaller particles (Fig. 6(*a*)). The particle size was obtained by the method of counting spots, and the results are given in Table 2. With increasing deformation, the particles became more distinct (Fig. 6(*b*)), and the particle size decreases until after about 10 % reduction a limiting particle size is reached.

The spread of spots into arcs implies that the material in the deformed grain covers a range of orientations. The lengths of the arcs, and hence the misorientations, increase with the degree of cold-work; but even in the heavily deformed material most of the spots lie within clearly defined arcs, thus showing that the particles are not randomly orientated (Fig. 5(*c*)). The total range of misorientations can be estimated from the length of the arc. If γ is the angle subtended by the arc at the centre of the ring, and β is the maximum angle between normals of the reflecting planes of two particles in the grain,

$$\sin \tfrac{1}{2}\beta = \cos\theta \sin \tfrac{1}{2}\gamma . \qquad (6)$$

The results are shown in Table 2. Since the X-ray photographs did not cover the same area of specimen, it is uncertain whether the increase of misorientations for the largest deformations can be regarded as significant.

The angles between particles giving adjacent spots were also obtained and are given in Table 2. These are found to increase with the degree of deformation (see also Fig. 6(*a*), (*b*)). A particular feature of the photographs of slightly deformed specimens (Fig. 5(*b*)) is that the mean radii are different for the various arcs. Moreover, the radius is found to vary continuously from one end of the arc to the other. This effect may be due to the possibilities that different parts of the grain have different mean strains, or that they are situated at slightly different positions in the area of cross-section of the beam. Whatever the reason for this effect, the fact that the variation across one arc is continuous, indicates that neighbouring spots are due to neighbouring particles in the grain. The angles between adjacent spots therefore give the angles between neighbouring particles.

For the heavily deformed material, the rings consist of clusters of several spots which appear to come from neighbouring parts of the grain; it is, however, impossible to decide whether adjacent groups of spots are due to adjacent parts of the grain. If the particles were randomly orientated the mean angle between adjacent particles should from statistical reasoning be $\sim \frac{1}{3}\times 16° \sim 5°$. If on the other hand the particles (2 μ) were regularly arranged as if they originated from polygonization of a uniformly bent grain (20 μ), the mean angle between particles should be $\sim \frac{2}{20}\times 16° \sim 1\frac{1}{2}°$. The evidence from the occurrence of groups of spots on the photographs suggests that this latter arrangement is more nearly correct, and the order of magnitude of the mean angle between particles is probably $\sim 2°$.

Table 2. *Particle size and misorientations of cold-worked spectroscopically pure aluminium*

Reduction (%)	Particle size (μ)	Angle between particles giving adjacent spots (′)	Total range of misorientations in original grain (°)
0	20	—	—
1·3	4·3	13	4
3	5·2	6	2
8	2·0	21	11
57	2·0	30	16

(a)

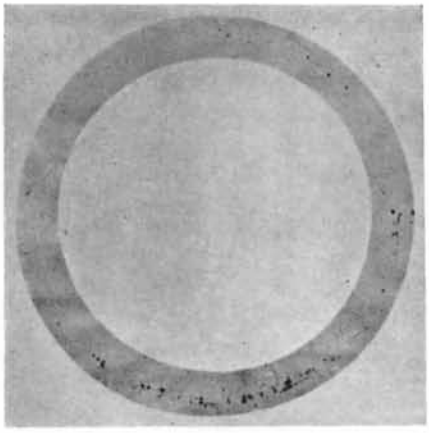

(c)

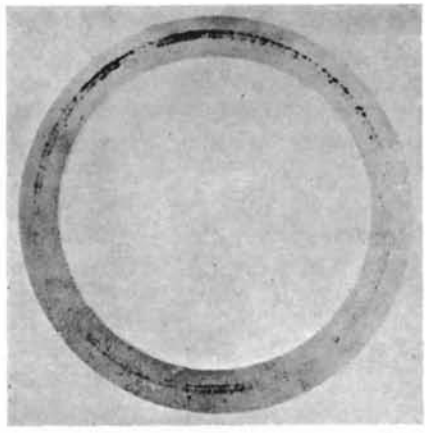

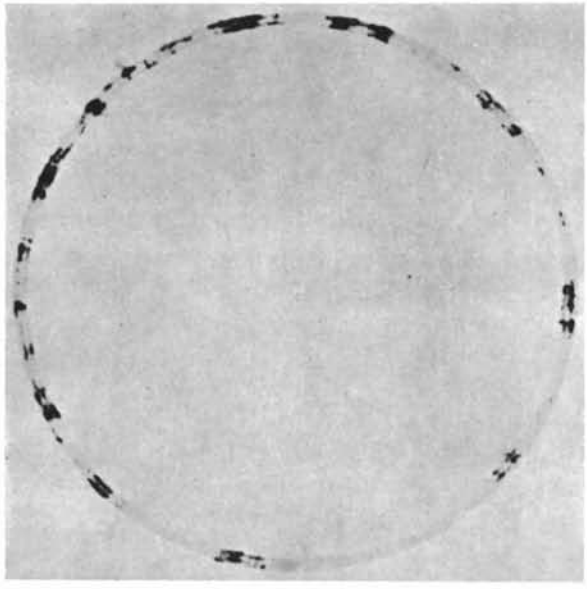

(b)

Fig. 5. Back-reflexion micro-beam photographs of the 422 reflexion from specimens of (*a*) annealed spectroscopically pure aluminium (150 μ diameter beam), (*b*) slightly rolled spectroscopically pure aluminium (150 μ diameter beam), (*c*) heavily rolled spectroscopically pure aluminium (35 μ diameter beam).

(a)

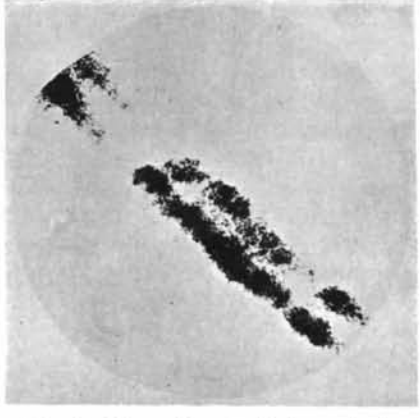

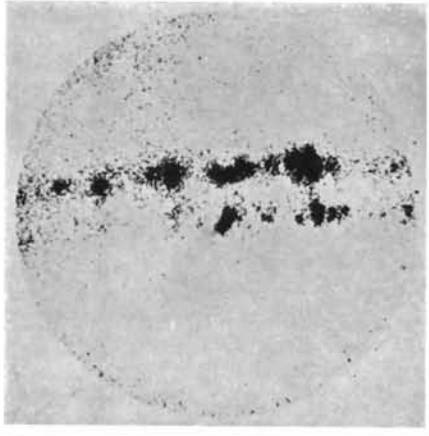

(b)

Fig. 6. Enlarged part of rings obtained from (*a*) slightly and (*b*) heavily deformed spectroscopically pure aluminium, showing the structure of the arcs.

[*To face p.* 166

9. Variation of particle size with time after rolling

For these experiments specimens of heavily rolled spectroscopically pure aluminium were used. The results are shown in Table 3 and show that the mean particle size decreases slightly with time after rolling.

Table 3. *Variation of particle size with time after rolling*

Reduction (%)	Time of examination after rolling	Particle size (μ)
57	14 days	2·6
	1 year	1·7
60	2 days	2·5
	4 months	2·2
	1 year	2·0

10. Effect of impurities

For these experiments specimens of commercially pure (99·2 %) aluminium were used, and the results are summarised in Table 4.

Table 4. *Effect of impurities.*

Reduction (%)	Particle size (μ)	Angle between particles giving adjacent spots (′)	Total range of misorientations in original grain (°)
0	20	—	—
6	4·1	11	2
72	$\sim$ 1·2	Impossible to estimate	$\sim$ 10

For small deformations the appearance of the pattern is little different from corresponding patterns for the spectroscopically pure material. Again the original spots spread into arcs which contain spots. However, a characteristic of all the photographs obtained was the poor resolution of the 'spots' within the arcs. This is especially marked for the heavily rolled material; photographs taken under the same conditions as for the spectroscopically pure material consist of rings of considerably weaker but more uniformly distributed blackening. This could be due to the following causes: (*a*) The mean particle size is smaller, and too many particles are illuminated. (*b*) The grain does not split into particles misorientated sufficiently to be resolved in the experiments.

Photographs were taken with smaller beams ($\sim$ 25 μ diameter at the specimen), smaller divergences, and longer exposures. So far, however, no photograph has been obtained showing clearly resolved spots. It is probable, therefore, that the relative misorientations are so small that spots from adjacent particles cannot be resolved. The limiting particle size (estimated approximately by counting the poorly resolved spots on the rings) is smaller than for the spectroscopically pure material.

Our thanks are due to Prof. Sir Lawrence Bragg and Dr W. H. Taylor for suggesting the problem and for their constant help and encouragement. We are grateful to our colleagues, P. Gay and J. S. Thorp for their help and advice, and to Mr G. C. Smith for providing the impure aluminium specimen. P. B. Hirsch acknowledges maintenance grants from the British Iron and Steel Research Association, and the Department of Scientific and Industrial Research, and a Junior Research Studentship from St. Catharine's College, Cambridge.

References

Bragg, W. L. (1948). *Proc. Camb. Phil. Soc.* **45**, 125.
Compton, A. H. & Allison, S. K. (1935). *X-rays in Theory and Experiment.* New York: Van Nostrand.
Hall, W. H. (1949). *Proc. Phys. Soc. Lond.* A, **62**, 741.
Hirsch, P. B. (1950). Ph. D. Dissertation, University of Cambridge.
Hirsch, P. B. (1952). *Acta Cryst.* **5**, 168.
Hirsch, P. B. & Kellar, J. N. (1951). *Proc. Phys. Soc. Lond.* B, **64**, 369.
Kellar, J. N., Hirsch, P. B. & Thorp, J. S. (1950). *Nature, Lond.* **165**, 554.
Megaw, H. D. & Stokes, A. R. (1945). *J. Inst. Metals*, **71**, 279.
Paterson, M. S. (1949). Ph. D. Dissertation, University of Cambridge.
Schdanow, H. S. (1935). *Z. Krystallogr.* **90**, 82.
Stephen, R. A. & Barnes, R. J. (1937). *J. Inst. Metals*, **60**, 285.
Wood, W. A. (1939). *Proc. Roy. Soc.* A, **172**, 231.